MEASUREMENT DISTANCE EFFECTS ON ϕ–SYMMETRIC SHAPED PATTERNS GENERATED BY CIRCULAR CONTINUOUS APERTURES

J. C. Brégains, F. Ares, and E. Moreno

Grupo de Sistemas Radiantes, Departamento de Física Aplicada,

Facultad de Física, Universidad de Santiago de Compostela.

15782 - Santiago de Compostela – Spain

faares@usc.es

http://aiff.usc.es/~fagsr

ABSTRACT

Sidelobe level and ripple behaviors of ϕ-symmetric shaped patterns -generated by circular, real and complex, Taylor continuous distributions- against measurement distances are analyzed. This paper reveals that real distributions suffer less significant power pattern degradation than complex at near-field distances.

1. INTRODUCTION

From a previous paper [1] it can be seen that circular continuous distributions generating Taylor sum patterns behave analogously to line sources [2]: the first sidelobe level change is represented as a straight line in a $\log_{10}(\Delta SLL)$ versus $\log_{10}$(measurement-distance) representation (being sidelobe level in dBs). This work shows, as in [3] (an analogous paper in which line sources are studied), that first sidelobe level in real circular distributions generating ϕ-symmetric shaped beams behaves like sum Taylor's, while ripple in the coverage zone almost maintains its far-field value. In contrast, in complex-valued continuous apertures the ripple zone is deeply degraded, and first sidelobe level change loses that linear behavior.

2. METHOD

The general continuous circular ϕ-symmetric expression in the Fresnel region is given by [1]:

$$F_\rho(\gamma,u)=\int_0^\pi g(\rho)\,\rho\,J_0(u\rho)\,e^{-j\frac{\rho^2}{8\pi\gamma}}d\rho \tag{1}$$

where $u = (2a/\lambda)\sin\theta$ (a being the radius of the circular aperture placed on x-y plane, λ the wavelength and θ the angle from the zenith), $\rho \in [0,\pi]$ is the normalized radius variable, $\gamma = R/R_0$, (R being distance from the antenna and R_0 the traditional far-field measurement distance, $8a^2/\lambda$). We set the aperture distribution $g(\rho)$ as:

$$g(\rho)=\frac{2}{\pi^2}\sum_{m=0}^{\bar{n}-1}\frac{F(\mu_{1m})}{J_0^2(\mu_{1m}\pi)}J_0(\mu_{1m}\rho) \quad \text{and} \quad F(u)=\frac{J_1(\pi u)}{\pi u}\prod_{n=1}^{\bar{n}-1}\frac{\left[1-\left(\frac{u}{u_n}\right)^2\right]}{\left[1-\left(\frac{u}{\mu_{1n}}\right)^2\right]}. \tag{2}$$

In this last expression, $\bar{n}$-1 is the number of pattern roots that are controlled on the far field pattern (since, with (2) and for large values of γ, eq. (1) approaches to the well known Taylor's far field expression $F(u)$ [1]) , u_n the n-th root of such pattern, and μ_{1m} (with m=0,1,2....), the first order first kind Bessel zeros divided by π, so as $J_1(\pi\mu_{1m})=0$.

In this work we used previously published methods to optimise real and complex apertures (by generalizing, for complex apertures, u_n to complex valued u_n+jv_n roots, and for real apertures, to complex roots consisting entirely on conjugated pairs) affording shaped beams with controlled far-field ripple and sidelobe levels [4,5], and investigated the dependence of the ripple and first sidelobe level change of these patterns against measurement distance (from near to far field values).

3. RESULTS

3.1. COMPLEX EXCITATIONS

To analyze shaped patterns provided by complex excitation distributions, we generated, setting $\bar{n}$ = 6, far-field rotationally symmetric shaped (flat topped) beam patterns with their three first ring sidelobes at -15, -20, -30 and -40 dB, filling two nulls so as to obtain ±0.50 dB of ripple in the coverage zone [4]. We achieved four aperture distributions (with radius a equal to 5λ) for each pattern, by changing the signs of the imaginary parts of the complex roots, since these changes do not modify the far-field power diagrams, while introduce significant degradations in near field ones, as it will be seen. Depending on the selected signs, the ripple zone suffers different morphological changes, and the deepness of the degradation is determined by the far field ripple value. To exemplify this behavior, similar in all the generated cases, Fig.1 shows power patterns at $\gamma = 0.5$ corresponding all of them to a far-field power diagram with ± 0.5 dB of ripple and -20 dB of sidelobe levels.

Plots of SLL changes versus γ were obtained to compare them with earlier results [1] obtained for rotationally symmetric sum patterns. In this sense, the most important conclusion is that the $\log_{10}[\Delta SLL]$-$\log_{10}[\gamma]$ representation is not a line for each given case. Figure 2 exemplifies these changes (ΔSLL-$\log_{10}[\gamma]$ representation) for cases with far-field sidelobe levels of -15, -20, -30 and -40 dB (represented all in cases with a ++ imaginary signs combination). Plots of ripple value versus γ remark the deep degradation of this parameter in near zone. Figure 3 illustrates the ripple with all possible combination of complex roots, and for a specific case of sidelobe level at -20 dB. All remaining patterns behave similarly, with a slight dependence of far field SLL value.

3.2. REAL EXCITATIONS

To obtain similar symmetric flat topped beams with real valued excitation distributions, we proceeded as in [5] filling the first four nulls (pairing two conjugated complex roots) in the coverage zone (setting $\bar{n}=8$). All generated cases demonstrated that ripple value is maintained almost undegraded in all γ range, while sidelobe level change has similar behavior as that of Taylor circular sum patterns [1].

4. CONCLUSIONS

Designers are allowed to select real-valued continuous circular distributions when flat topped beams with the lowest degradation at near field are needed, because they maintain ripple close to far field value, and first sidelobe level rises as in Taylor sum pattern. For complex-valued apertures, a minimum 10 R_0 distance is needed to guarantee that these parameters are close enough to far-field values, since they suffer deep degradations at distances closer to the aperture.

5. ACKNOWLEDGEMENT

This work was supported by the Spanish Ministry of Science and Technology under project TIC 2002-04084-C03-02

6. REFERENCES

[1] P. Corona, G. Ferrara, and C. Gennarelli, "Measurement Distance Requirements for Both Symmetrical and Antisymmetrical Aperture Antennas", IEEE Trans. On Antennas and Propagat., **AP- 37**, 8, August 1989, pp. 990-995.

[2] R. C. Hansen, "Measurement Distance Effects On Low Sidelobe Patterns", IEEE Trans. On Antennas and Propagat., **AP- 32**, June 1984, pp. 591-594.

[3] J. C. Brégains, F. Ares and E. Moreno, "Effects Of Measurement Distance On Measurements Of Symmetric Shaped Patterns Generated By Line Sources", IEEE Antennas and Propagation Magazine, **45**, 1, February 2003, pp. 106-109.

[4] R. S. Elliott, and G. J. Stern, "Shaped Patterns From a Continuous Planar Aperture Distribution", IEE Proceedings, Pt. H., **135**, 6, December 1988, pp. 366-370.

[5] R. S. Elliott, and G. J. Stern, "Footprint Patterns Obtained by Planar Arrays", IEE Proceedings, Pt. H, **137**, 2, April 1990, pp. 108-112.

LEGENDS FOR THE FIGURES

Figure 1. Power patterns at a distance of $\gamma = 0.5$ generated by complex circular apertures synthesized to generate the indicated shaped ϕ-symmetric far-field pattern. Patterns A, B, C and D correspond to the combinations of the signs of the imaginary parts of the two complex roots of the pattern (A, ++; B, --; C, +-; D, -+).

Figure 2. First sidelobe level change (relative to the far-field first sidelobe level) against measurement distance of shaped ϕ-symmetric patterns generated by complex circular apertures synthesized to get far-field patterns with ± 0.5 dB of ripple and -15, -20, -30 or -40 dB first sidelobe levels (all for case A of Fig.1). The arrows indicate shoulders.

Figure 3. Ripple of shaped symmetric patterns generated by complex line sources synthesized to afford far-field patterns with ± 0.5 dB of ripple and -20 dB first sidelobe levels. Patterns shown are for the same cases of Fig.1.

<table>
<tr><th>CASE</th><th>POWER
PATTERN</th></tr>
<tr><td>A, B</td><td>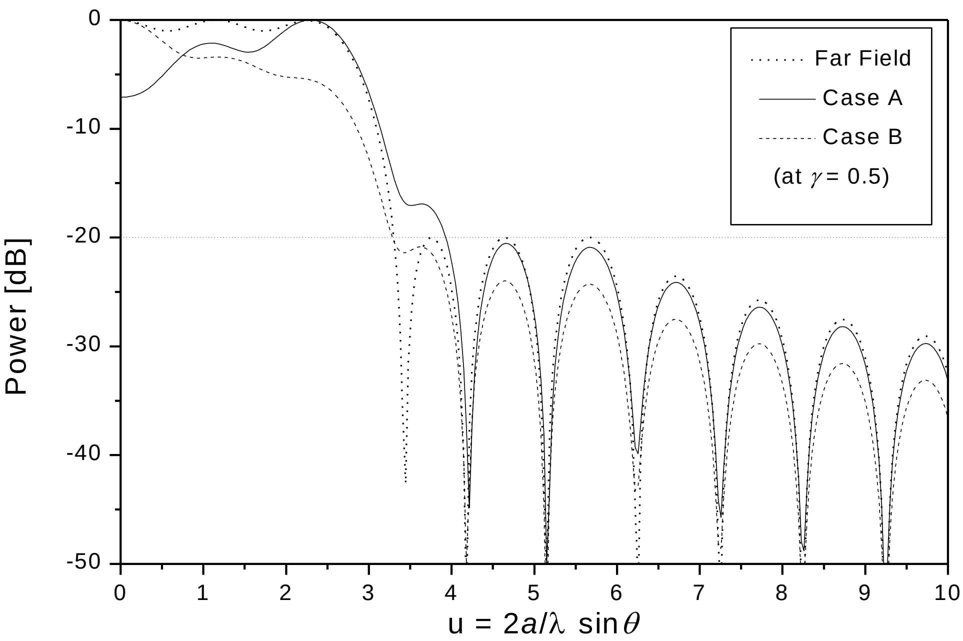
</td></tr>
<tr><td>C, D</td><td>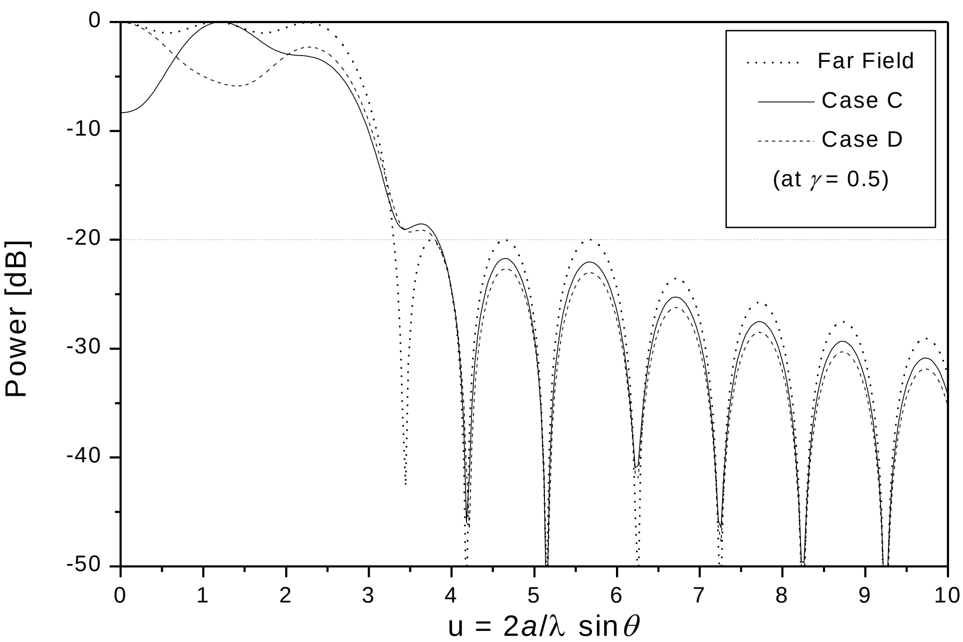
</td></tr>
</table>

Figure 1

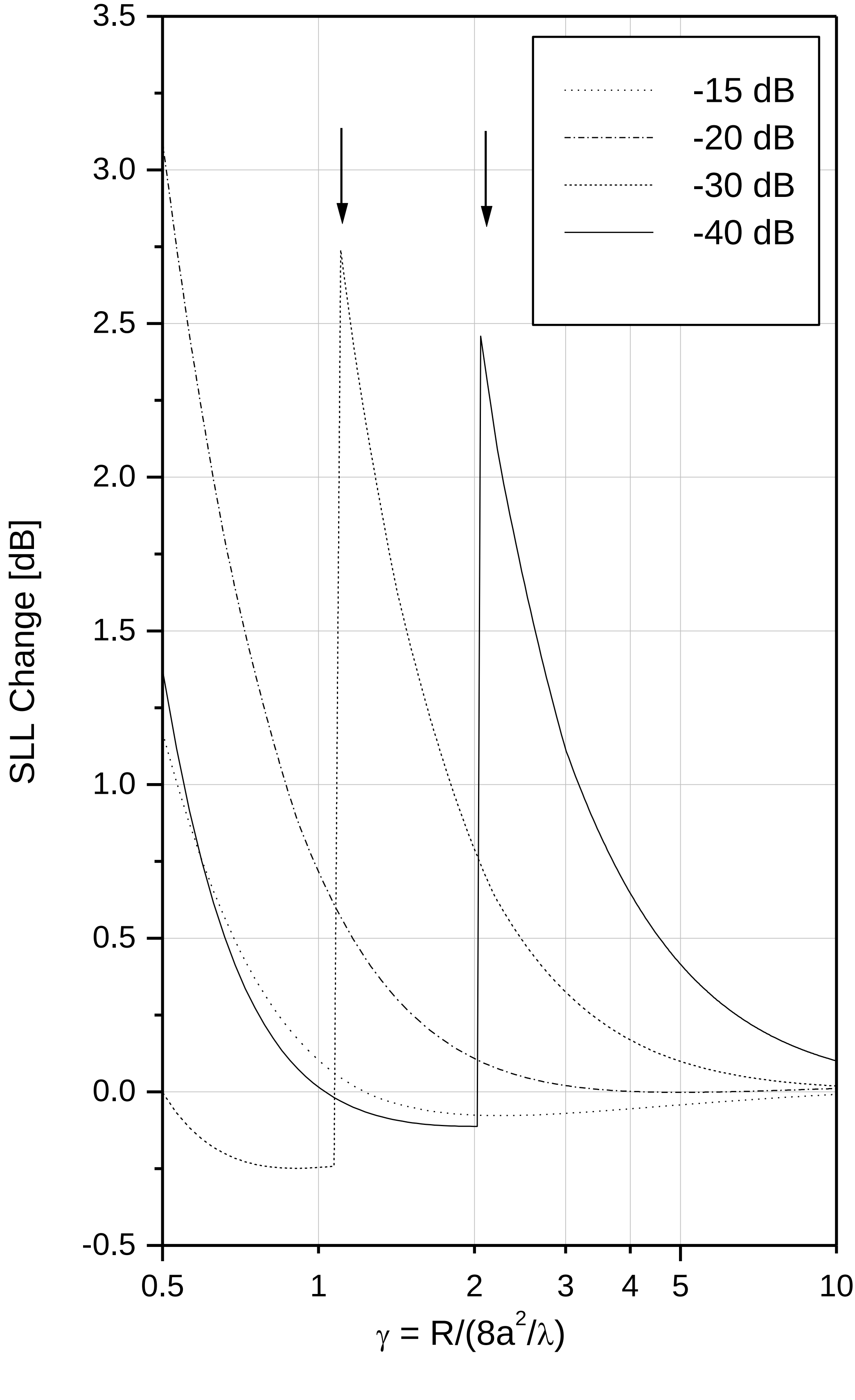
-15 dB
-20 dB
-30 dB
-40 dB
SLL Change [dB]
3.5
3.0
2.5
2.0
1.5
1.0
0.5
0.0
-0.5
0.5
1
2
3
4
5
10
γ = R/(8a²/λ)

Figure 2

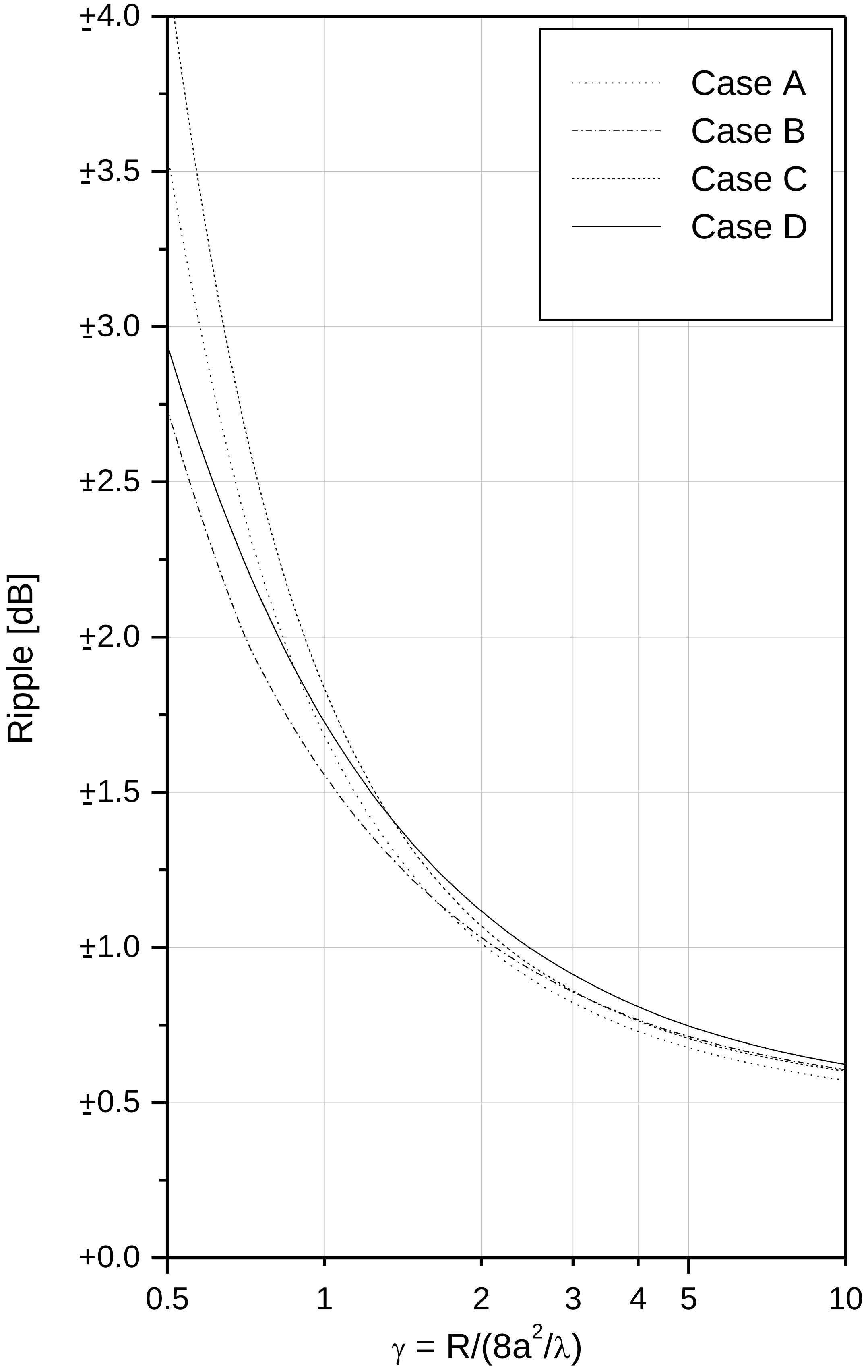

Case A
Case B
Case C
Case D
Ripple [dB]
±4.0
±3.5
±3.0
±2.5
±2.0
±1.5
±1.0
±0.5
+0.0
0.5
1
2
3
4
5
10
γ = R/(8a²/λ)

Figure 3